Applied Catalysis B: Environmental 147 (2014) 369–376

Contents lists available at ScienceDirect

Applied Catalysis B: Environmental

journal homepage: www.elsevier.com/locate/apcatb

Electrocatalytic oxygen reduction on nitrogen-doped graphene in alkaline media

Merilin Vikkisk[a], Ivar Kruusenberg[a], Urmas Joost[b], Eugene Shulga[b], Ilmar Kink[b], Kaido Tammeveski[a,*]

[a] Institute of Chemistry, University of Tartu, Ravila 14a, 50411 Tartu, Estonia
[b] Institute of Physics, University of Tartu, Riia 142, 51014 Tartu, Estonia

ARTICLE INFO

Article history:
Received 19 June 2013
Received in revised form 4 September 2013
Accepted 9 September 2013
Available online 19 September 2013

Keywords:
Graphene
Nitrogen doping
Oxygen reduction
Electrocatalysis
Alkaline membrane fuel cell

ABSTRACT

Nitrogen-doped graphene nanosheets were prepared from nitrogen precursor and graphene oxide (GO), which was synthesised from graphite by modified Hummers' method. Melamine, urea and dicyandiamide (DCDA) were used as nitrogen precursors and the doping was achieved by pyrolysing GO in the presence of these nitrogen-containing compounds at 800 °C. The N-doped graphene (NG) samples were characterised by scanning electron microscopy and X-ray photoelectron spectroscopy, the latter method revealed successful nitrogen doping. The oxygen reduction reaction (ORR) was examined on NG-modified glassy carbon (GC) electrodes in alkaline media using the rotating disk electrode (RDE) method. It was found on the basis of the RDE results that nitrogen-containing catalysts possess higher electrocatalytic activity towards the ORR than the annealed GO. Oxygen reduction on this GO material and on NG catalysts prepared by pyrolysis of GO-melamine and GO-urea followed a two-electron pathway at low overpotentials, but at higher cathodic potentials the desirable four-electron pathway occurred. For NG catalyst prepared from GO-DCDA a four-electron O_2 reduction pathway dominated in a wide range of potentials. The half-wave potential of O_2 reduction on this NG catalyst was close to that of Pt/C catalyst in 0.1 M KOH. These results are important for the development of alkaline membrane fuel cells based on non-platinum cathode catalysts.

1. Introduction

Nowadays mainly Pt and Pt-based catalysts have been employed as cathode catalysts in low-temperature fuel cells. Because of the high price and scarcity of Pt, a great deal of work has been made to develop new electrocatalysts for oxygen reduction reaction (ORR) in alkaline and acidic media. In order to replace platinum, different carbon-based materials that possess lower price, better availability and improved chemical stability have been studied [1–4]. It is well known that the greater the extent of graphitisation of the carbon material, the better its durability [5]. Few-layer graphene, its characteristics and production is attracting as much attention as carbon nanotubes (CNTs) received during the last decade [6]. Despite the fact that CNTs have unique structure and high electrical conductivity, their electrochemical performance is still suffered due to their low stability against oxidation by peroxide intermediates leading to fuel cell catalyst degradation [7]. In addition, comparing to alkaline media, CNT-based catalysts show lower activity towards the ORR in acids [8–11]. These might be few reasons why there has been an immense research activity in the search for alternative carbon materials for ORR [4].

Graphene is a flexible and expandable two-dimensional (2D) monolayer carbon material consisting of sp^2 carbon atoms [12,13]. It is an attractive material thanks to several features: the unique chemistry of the edges of a graphene sheet, the mechanical strength, high thermal and chemical stability, high electrical conductivity and large surface area [6,12–16]. Graphene has been used in various electrochemical applications like batteries, fuel cells, electrochemical energy storage and supercapacitor electrodes due to its high electrical conductivity and remarkable electronic properties [17,18]. Because of these promising applications a facile, environmentally friendly and cost-effective method for mass production of graphene is needed [19]. The most promising graphene synthesis method is based on the reduction of graphene oxide (GO), where graphite is chemically exfoliated into GO, followed by chemical or thermal elimination of oxygen groups [20].

Recently, Zhu and Dong reviewed the application of graphene-based electrocatalysts for ORR [21]. Nitrogen-doped carbon materials have been considered as promising cathode catalysts for low-temperature fuel cells [22,23]. For the chemical doping

* Corresponding author. Tel.: +372 7375168; fax: +372 7375181.
E-mail addresses: kaido.tammeveski@ut.ee, kaido@chem.ut.ee (K. Tammeveski).

0926-3373/$ – see front matter © 2013 Elsevier B.V. All rights reserved.
http://dx.doi.org/10.1016/j.apcatb.2013.09.011

of carbon materials, nitrogen is considered to be an excellent choice, because it has comparable atomic size with carbon and it forms strong bonds with carbon atoms. The lone electron pairs of nitrogen atoms can form a delocalised conjugated system with the sp^2-hybridised carbon frameworks, which improves the reactivity and electrocatalytic performance of graphene [24]. Sheng et al. reached nitrogen level up to 10% in the N-doped graphene (NG) material and the obtained catalyst exhibited an outstanding performance for O_2 reduction in fuel cell [25]. Nitrogen atoms can donate electrons to the conjugated π orbital in carbon, polarising the C atoms into C (δ+), making it easy to adsorb the O_2 molecule and also helping to form a strong chemical bond between C and O, which splits the O–O bond [14,26]. Introducing abundant defects is another possible approach to enhance the ORR activity [7]. It is well known that the electrocatalytic activity of nitrogen-doped graphene is related not only to the nitrogen level, but also to the type of nitrogen [21]. Typically, the NG catalysts consist of different types of N-containing groups. This makes it difficult to interpret the electrocatalytic behaviour of NG towards the ORR, because one cannot unequivocally relate the ORR activity to a certain type of N sites. According to XPS analysis, the following types of nitrogen have been detected in N-doped carbon materials: pyridinic N, quaternary N (graphitic N), pyrrolic N and pyridine-N-oxide [22,23]. Some research groups have claimed that the graphitic nitrogen is responsible for the high ORR activity and the other N functionalities that mainly exist on the edges of NG have smaller impact [27]. Others state that pyridinic N and the small pores of the catalyst are responsible for electrocatalysis of the ORR [28]. Which type of C–N bonding configuration is responsible for improved electrocatalytic activity is still under the debate [21].

Several groups have reported that NG possesses excellent electrocatalytic activity towards the ORR in alkaline media, but in acid the activities comparing to Pt/C catalyst are much lower [25,29–31]. It also needs to be stressed that NG is more stable than Pt/C during accelerated degradation test and it shows significantly better tolerance towards methanol and CO. This is particularly attractive for low-temperature fuel cell application [21].

For nitrogen doping, there are different opportunities including chemical and physical synthesis and each method creates doped graphene with different characteristics. Chemical vapour deposition (CVD) is capable of producing high-quality N-doped graphene sheets, but suffers from complicated equipment, high cost and is not suitable for mass production [32]. Nitrogen species can be incorporated into graphene by annealing of GO in ammonia [32]. Thermal decomposition method has been frequently employed for the preparation of nitrogen-doped graphene [22]. Various nitrogen precursors were used for the high temperature pyrolysis in the presence of GO. Urea has also served as an expansion–reduction agent for graphene generation [6,16]. The use of an expansion-reducing agent will not only create volatile species that mechanically expand GO, but will also allow the volatile gases to reduce oxygen-containing groups on the surface of GO, which is favourable for incorporating nitrogen into graphene structure [6,16].

Recently, we have studied the reduction of oxygen on N-doped CNTs prepared by CVD [33] and by post-deposition treatment of CNTs with urea [34]. Both materials showed high ORR activity in alkaline media. In current work, we synthesised nitrogen-doped graphene via reducing GO with three different nitrogen-containing compounds (dicyandiamide, urea and melamine) by high-temperature pyrolysis in an inert atmosphere. By controlling the experimental conditions, including pyrolysis temperature and mass ratio between GO and nitrogen precursor, the overall content and type of nitrogen could be modified. The electrochemical reduction of oxygen has been studied on NG materials in alkaline media using linear sweep voltammetry and the rotating disk electrode method.

2. Experimental

2.1. Preparation of graphene oxide (GO)

GO is a highly oxidised form of graphene and contains many carbon–oxygen functionalities on the surface, for example carboxylic, carbonyl, epoxy and hydroxyl groups [35]. GO is well dispersed in water, because the oxygen-containing groups are hydrophilic and carboxyls bring negative charges to the GO surface [35]. The GO material used in this work was synthesised from graphite powder (Graphite Trading Company) by a modified Hummers' method [15,36]. Firstly, 50 ml of concentrated sulphuric acid and 2.0 g of graphite powder were mixed in a 250 ml beaker at room temperature. Then, the mixture was sonicated for 1 h. Next, sodium nitrate (2.0 g) and potassium permanganate (6.0 g) divided to smaller portions were slowly added into the beaker in a sequence. At the same time the mixture was stirred on a magnetic stirrer. Afterwards, the mixture was heated at 35 °C for 18 h. When the heating was completed, the beaker was put into an ice bath and 80 ml of deionised water was added into the solution. Few minutes later, 20 ml of H_2O_2 (30%) was added. The mixture was then washed few times with 10% HCl solution and with water on a vacuum filter. Finally, the obtained brown solid was dried in vacuum at 75 °C.

2.2. Synthesis of N-doped graphene (NG)

Three different precursors were used for nitrogen doping. Melamine, urea and dicyandiamide (DCDA) were all purchased from Aldrich. Firstly, GO and some polyvinyl pyrrolidone (PVP) were dispersed in deionised water and after that nitrogen precursor was added. To compare different materials, GO/melamine, GO/urea and GO/DCDA with ratio 1/20 were prepared. These materials are designated as 1-NG, 2-NG and 3-NG, respectively. All the mixtures were sonicated for 2 h and after that dried at 75 °C in vacuum. Next, the materials were pyrolysed in flowing argon atmosphere at 800 °C for 2 h. After maintaining the temperature for 2 h, the furnace was cooled to room temperature and the final black product was collected. In order to compare the properties of undoped substrate in the same conditions the synthesised GO material was annealed in inert atmosphere at 800 °C for 2 h prior to electrochemical testing.

2.3. Surface characterisation of NG samples

The surface morphology of NG materials was examined with scanning electron microscope Helios^{TM} NanoLab 600 (FEI). For the morphological characterisation, Si plate served as the substrate material. To assess material's average characteristics, many different areas of the sample were observed. X-ray photoelectron spectroscopy (XPS) was used to analyse the surface composition of N-doped materials. NG suspensions in 2-propanol (3 mg ml^{-1}) were pipetted onto Si plates (1.1 × 1.1 cm) and then the plates were dried in an oven at 80 °C until the entire solvent was evaporated. The XPS analysis was carried out with SCIENTA SES-100 spectrometer. The materials were studied with a non-monochromatic twin anode X-ray tube (XR3E2) with characteristic energies of 1253.6 eV (Mg $K\alpha_{1,2}$, FWHM 0.68 eV) and 1486.6 eV (Al $K\alpha_{1,2}$ FWHM 0.83 eV). A source power of 300 W was used and the pressure in the analysis chamber was below 10^{-9} Torr. To collect the survey scan the following parameters were used: energy range = 800 to 0 eV, pass energy = 200 eV, step size = 0.5 eV. For high resolution scans in specific regions pass energy of 200 eV and step of 0.1 eV were used.

2.4. Electrode preparation and electrochemical measurements

The rotating disk electrode (RDE) method was used to perform the oxygen reduction measurements. The electrode rotation rate (ω) was varied from 360 to 4600 rpm. The RDE was equipped with CTV101 speed control unit and EDI101 rotator (Radiometer). Linear sweep voltammetry (LSV) was also used for the O_2 reduction studies. Electrochemical experiments were carried out at room temperature (23 ± 1 °C) in 0.1 M KOH solution (p.a. quality, Merck) in a three-electrode electrochemical cell. For electrochemical measurements the solutions were saturated with O_2 (99.999%, AGA) or Ar (99.999%, AGA). During the experiments the gas flow was maintained over the solution. Saturated calomel electrode (SCE) served as a reference electrode and all the potentials are referred to this electrode. Pt foil served as a counter electrode and was separated from the solution with a glass frit. The potential was applied to electrodes using Autolab potentiostat/galvanostat PGSTAT30 (Eco Chemie B.V., The Netherlands) and General Purpose Electrochemical System (GPES) software was used to control the experiments.

Glassy carbon (GC) was used as a substrate material. GC disks (GC-20SS, Tokai Carbon) with geometric area (A) of 0.2 cm^2 were pressed into a Teflon holder and the electrodes were polished to a mirror finish with 1 and 0.3 μm alumina slurries (Buehler). After polishing, the electrodes were sonicated in 2-propanol and Milli-Q water for 5 min. The GC disk electrodes were modified with NG aqueous suspensions (1 mg ml^{-1}) containing Tokuyama OH^- ionomer AS-04 (0.25%). The NG suspensions were sonicated for 1 h prior electrode modification. After that a 20 μl aliquot of the suspension was pipetted onto the GC surface and was allowed to dry in air. Care was taken to cover the surface of GC uniformly with catalyst layer.

For comparison purposes the reduction of oxygen was also studied on Pt/C catalysts deposited on GC. The commercial 20 wt% Pt catalyst supported on Vulcan XC-72 carbon was purchased from E-TEK, Inc. (Frimingham, MA, USA) and dispersed in ethanol (1 $mg_{catalyst}$ ml^{-1}). The Pt loading was 20 μg cm^{-2} of geometric electrode area.

3. Results and discussion

3.1. Surface morphology and XPS analysis of NG samples

The surface morphology of NG and GO samples was characterised by scanning electron microscopy (SEM). A drop of aqueous suspension of these materials was applied onto the Si substrate and the SEM micrographs of the NG catalyst and undoped GO are shown in Fig. 1. The NG layer contains micron-sized flakes and three dimensional (3D) particles that have size of hundreds of nanometers. Typical graphene structure (crumpled sheet-like morphology and porous architecture) revealing a high exfoliation degree is in evidence (Fig. 1a). No larger amorphous carbon particles or other impurities are visible on the image. Graphene nanosheets as two-dimensional materials tend to stack together through π–π interactions, which causes the blocking of catalytically active sites on the NG catalysts [21]. Further efforts need to be made to decrease the electrochemical deactivation caused by the stacking on the surface. For comparison purposes the SEM image of undoped GO material is presented in Fig. 1b. As can be seen from these two SEM images, no major change in the surface morphology occurred during the N-doping.

The elemental composition and chemical surrounding of N species in N-doped graphene materials was characterised by X-ray photoelectron spectroscopy. In the wide scan spectrum of annealed GO only C1s and O1s XPS peaks are present (data not shown). For NG samples also N1s peak appears. The high-resolution C1s peak

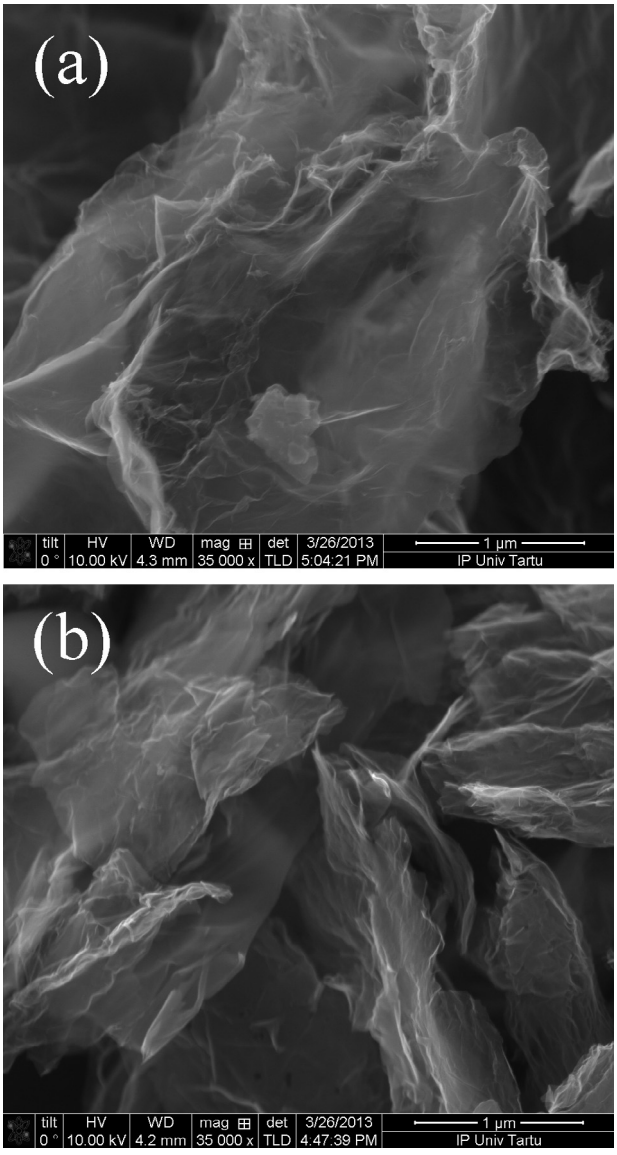

Fig. 1. SEM images of (a) nitrogen-doped graphene and (b) undoped GO.

appears at 284.8 eV, O1s at 532.1 eV and N1s at 398.2 eV. The high resolution spectra in the C1s region (Fig. 2) indicate the presence of different species: C=C (284.6 eV), C–C (285.5 eV), C=N (285.5 eV), C–O (286.6 eV) and O–C=O (288.1 eV) [25,26,37]. Different carbon-oxygen functionalities are present on the NG surface. It is suggested that majority of oxygen is removed below 400 °C by pyrolysis of the oxygen-containing functional groups [38,39]. This oxygen species removal process might provide active sites for nitrogen doping into graphene framework [25]. In the high resolution N1s spectrum (Figure 2), the peak can be deconvoluted into four components: quaternary N (401 eV), pyrrolic N (400 eV), pyridinic N (398 eV) and pyridine-N-oxide (403 eV). The quaternary nitrogen corresponds to N atoms that are linked with three carbon atoms in graphene basal plane, replacing the C atoms in graphene hexagonal ring [22,23]. Pyrrolic N occurs in five-member ring and can contribute to the π-conjugated system in the graphene layers with two p-electrons [25]. Pyridinic N occurs in six-member ring and can donate one p-electron to the aromatic π system [25]. The total nitrogen content in 1-NG was 5 at%, from which pyridinic N constitutes 33 at%, quaternary N 15 at%, pyrrolic N 26 at% and pyridine-N-oxide 25 at%. In 2-NG samples the overall N content was found to be approximately 3 at%, from which pyridinic N constitutes 42 at%, quaternary

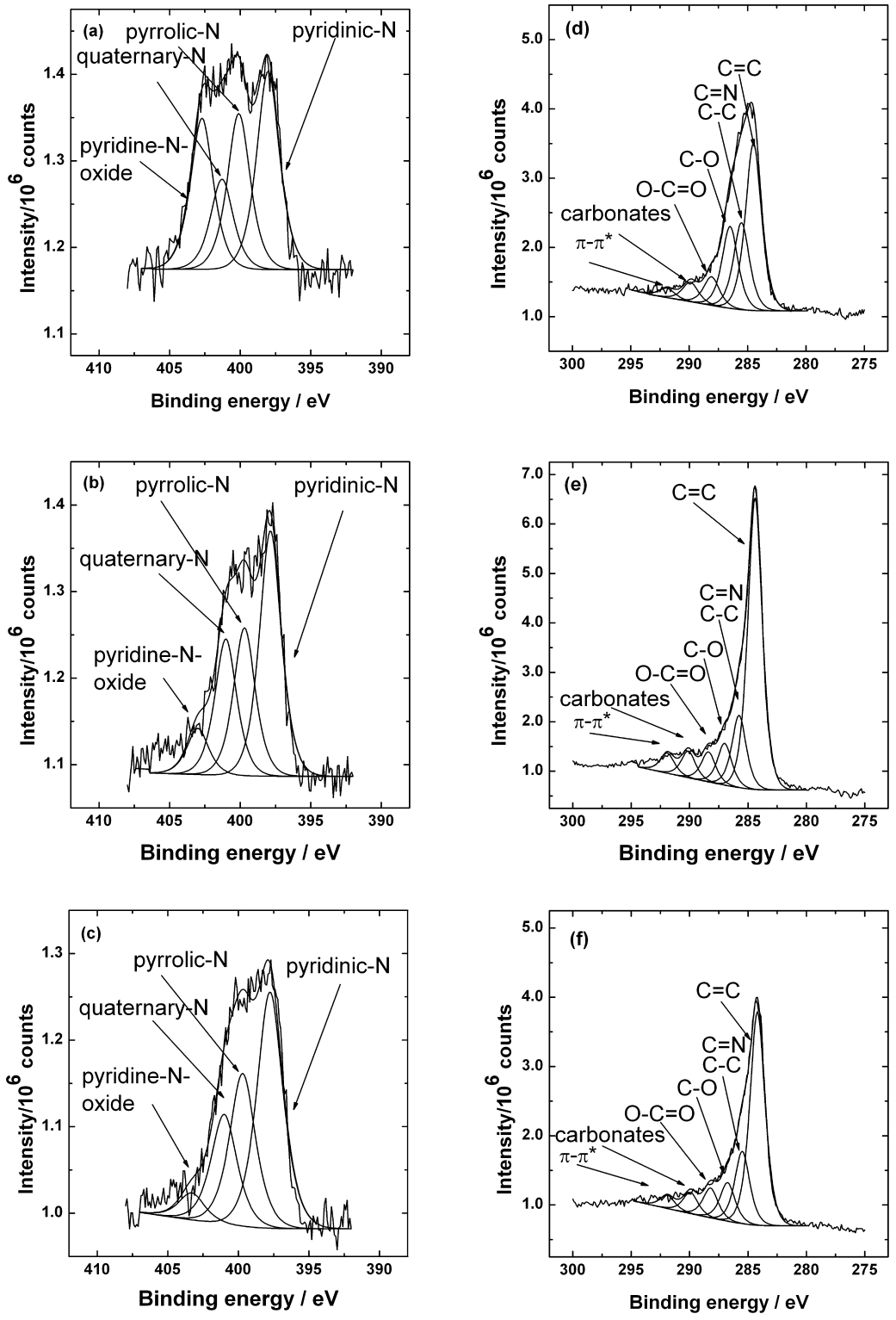

Fig. 2. High-resolution XPS spectra of NG samples in the N1s and C1s regions ($h\nu$ = 1253.6 eV, scan step 0.1 eV). The NG catalysts were prepared by pyrolysing (a), (d) GO–melamine, (b), (e) GO–urea and (c), (f) GO–DCDA at 800 °C for 2 h.

N 24 at%, pyrrolic N 26 at% and pyridine-N-oxide 8 at%. The overall N content in 3-NG samples was found to be ca. 5 at%, from which pyridinic N constitutes 45 at%, quaternary N 21 at%, pyrrolic N 29 at% and pyridine-N-oxide 5 at%. The XPS analysis clearly shows that nitrogen doping was successful and four different N-type species were present, from which the main component is pyridinic nitrogen.

3.2. Oxygen reduction in alkaline media

In this work the electrocatalytic activity of different graphene-based catalysts towards the ORR was explored. Graphene oxide was prepared from graphite powder and for nitrogen doping melamine, urea and DCDA were used. First, the electrocatalytic properties of undoped GO annealed at 800 °C were investigated in 0.1 M KOH

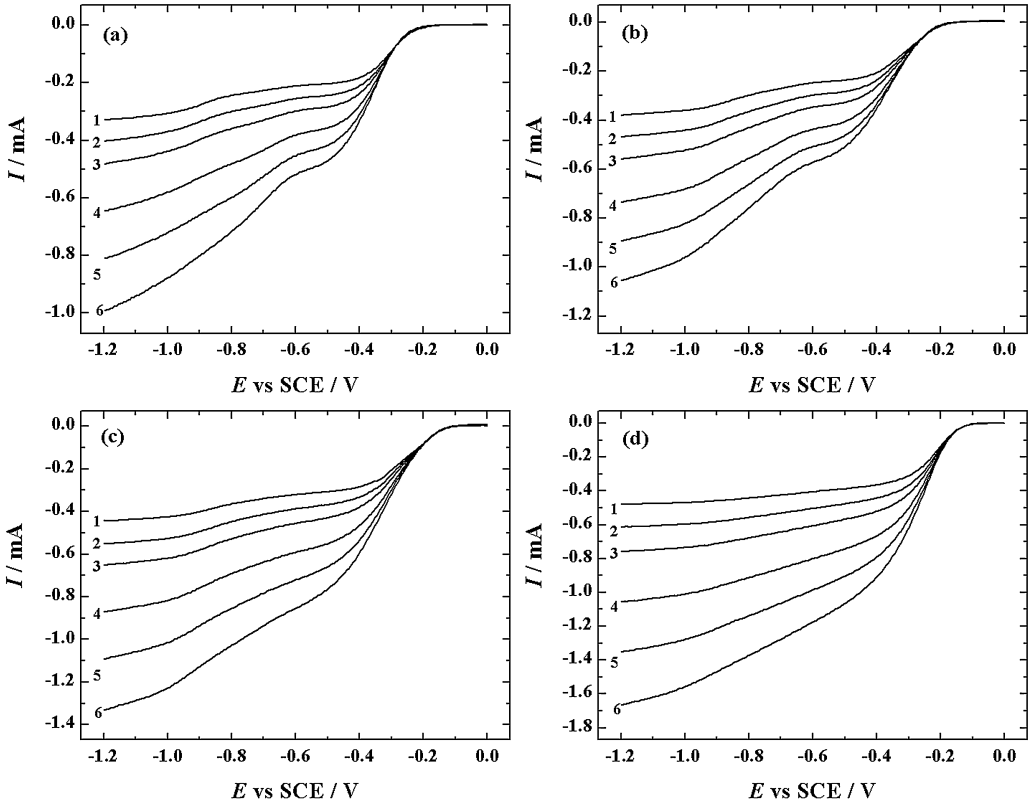

Fig. 3. RDE voltammetry curves for oxygen reduction on (a) GO, (b) 1-NG, (c) 2-NG and (d) 3-NG modified GC electrodes in O_2-saturated 0.1 M KOH. $\nu = 10\,mV\,s^{-1}$, ω = (1) 360, (2) 610, (3) 960, (4) 1900, (5) 3100 and (6) 4600 rpm.

solution using the RDE method. Fig. 3a shows the RDE results of O_2 reduction obtained with GO/GC electrode. The annealed GO catalyst shows rather good electrocatalytic activity for O_2 reduction. The onset potential of the ORR for this material is approximately −0.2 V and at higher negative potentials (ca. −0.6 V) a second reduction wave commences, which is in agreement with previous reports [25]. Similar RDE results of oxygen reduction have been obtained with GO modified GC recently [40,41].

The number of electrons transferred per O_2 molecule (n) was calculated from the Koutecky–Levich (K–L) equation [42]:

$$\frac{1}{I} = \frac{1}{I_k} + \frac{1}{I_d} = -\frac{1}{nFAkc^b_{O_2}} - \frac{1}{0.62nFAD^{2/3}_{O_2}\nu^{-1/6}c^b_{O_2}\omega^{1/2}} \quad (1)$$

where I is the measured current, I_k and I_d are the kinetic and diffusion-limited currents, respectively, k is the rate constant for O_2 reduction, A is the geometric electrode area, F is the Faraday constant (96485 C mol^{-1}), ω is the rotation rate (rad s^{-1}), D_{O_2} is the diffusion coefficient of oxygen (1.9×10^{-5} cm^2 s^{-1}) [43], ν is the concentration of oxygen in the bulk (1.2×10^{-6} mol cm^{-3}) [43] and ν is the kinematic viscosity of the solution (0.01 cm^2 s^{-1}) [44].

The K–L plots of oxygen reduction on the GO/GC electrode and the potential dependence of n are presented in Fig. 4a. The number of electrons transferred per O_2 molecule at low overpotentials is close to two and at more negative potentials the value of n reaches 2.8. This shows that at low overpotentials the ORR follows a 2e$^-$ process with the formation of HO_2^-, but at more negative potentials the formed peroxide partly reduces further. The extrapolation of the K–L lines yields an intercept that is quite large even at −1.2 V. This shows that the process of O_2 reduction is under the mixed kinetic-diffusion control in a wide range of potentials.

Next, the electrocatalytic properties of different nitrogen-containing materials were examined. The polarisation curves of oxygen reduction on the 1-NG catalyst (prepared by pyrolysis from GO-melamine mixture) are shown in Fig. 3b. The O_2 reduction wave starts approximately at −0.2 V and the process is under the mixed kinetic-diffusion control in the whole range of potentials. The K–L plots of oxygen reduction on the 1-NG catalyst are presented in Fig. 4b. The K–L lines are linear and the value of n derived from the slope of these lines is ca. 2.5 at lower overpotentials and reaches 3.4 at more negative potentials. The value of n for GO-melamine catalyst has also been found to be around 3 by other groups [25,35].

Fig. 3c and d shows the O_2 reduction polarisation curves for 2-NG (GO-urea) and 3-NG (GO-DCDA) modified GC electrodes in O_2-saturated 0.1 M KOH. Compared with annealed GO and 1-NG materials, the ORR onset potential of 2-NG and 3-NG shifts positive and the O_2 reduction current is also larger, indicating faster electron transfer kinetics for ORR. For 3-NG modified GC electrode diffusion-limited current plateaus are formed at low rotation rates, but at higher rates the process of O_2 reduction is under the mixed kinetic-diffusion control.

The oxygen reduction wave commences at −0.15 and −0.12 V for 2-NG and 3-NG materials, respectively. The latter material shows almost 100 mV positive shift in the onset potential compared with annealed GO indicating its enhanced electrocatalytic activity. The K–L plots and the potential dependence of n are shown in Fig. 4c and d. For 2-NG the value of n at low overpotentials is close to 3 and at more negative potentials ca. 3.8. Wu et al. also synthesised NG catalyst from GO and urea and this catalyst exhibited high electrocatalytic activity for ORR, showing the n value higher than 3 at low overpotentials [45]. For 3-NG catalyst the value of n is 3.5 at low overpotentials and approximately four at more negative potentials. These n values are slightly lower than that of state-of-the-art Pt/C catalysts, which shows that at low overpotentials some peroxide is produced and at higher cathodic potentials 4e$^-$ reduction occurs.

In a recent work Zhang et al. [46] reported a hydrothermal procedure for the synthesis of NG material in an aqueous suspension of GO containing DCDA by heating at 180 °C in an autoclave. These

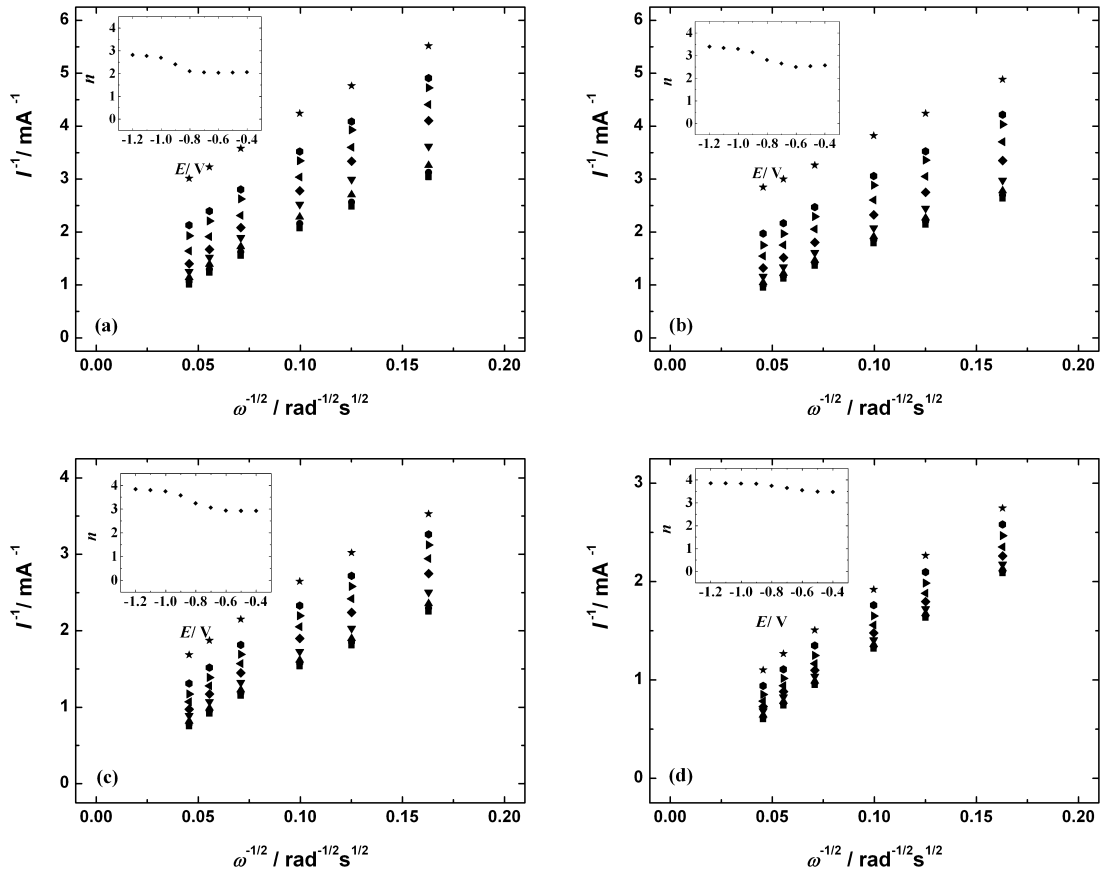

Fig. 4. Koutecky–Levich plots for oxygen reduction on (a) GO/GC, (b) 1-NG/GC, (c) 2-NG/GC and (d) 3-NG/GC electrodes in 0.1 M KOH solution. E = (⋆) −0.4, (●) −0.5, (►) −0.6, (◄) −0.7, (♦) −0.8, (▼) −0.9, (▲) −1.0, (●) −1.1 and (■) −1.2 V. Inset shows the potential dependence of n. Data derived from Fig. 3.

authors reported that the O_2 reduction wave on reduced GO and N-doped graphene commences at the same potential. For the latter material the n value was only 2.6 at −0.5 V vs. Ag/AgCl, which shows that peroxide pathway dominates on that NG catalyst. In the present research the reduction current was significantly larger on the 3-NG catalyst and the process of O_2 reduction proceeded by a 4-electron pathway, which indicates about the superiority of the NG catalyst used in this work. Obviously the high-temperature pyrolysis yields a more active catalyst for ORR than a wet chemical procedure suggested in Ref. [46].

The RDE results of O_2 reduction that compare the undoped GO and different NG catalysts at a single electrode rotation rate (ω = 1900 rpm) are shown in Fig. 5. The onset potential for all NG materials is higher compared with the annealed GO material. The catalyst prepared by the pyrolysis of the mixture of GO and DCDA with ratio of 1/20 (designated as 3-NG) shows the largest O_2 reduction current and the highest electrocatalytic activity. Compared with 1-NG and 2-NG, the ORR activity of 3-NG is significantly enhanced. Which type of nitrogen is responsible for improved ORR performance is not exactly known [14], but it is obvious on the bases of these results that incorporating nitrogen into carbon materials is necessary to obtain catalyst with better electrocatalytic properties. The investigation of oxygen molecule dissociation energy barrier has shown that it can be reduced by all types of nitrogen and the quaternary N reduces the energy barrier more efficiently than the pyridinic N, which might be one of the reasons for improved electrocatalytic activity on N-doped carbon catalysts [47]. Ruoff and co-workers stated that the content of graphitic N determines the electrocatalytic activity and pyridinic N is responsible for improving the onset potential and converting the ORR mechanism from 2-electron pathway to 4-electron process [48]. Some investigators claim that quaternary nitrogen is responsible for the enhanced catalytic activity, but some others state that it is the pyridinic nitrogen [27,28]. On the basis of the results obtained in this work, we conclude that the main reason for enhanced electrocatalytic activity of these electrocatalysts could be the higher content of pyridinic nitrogen. The 3-NG material possessed the highest ORR activity and this particular NG catalyst consisted of largest amount of pyridinic nitrogen. At the same time the 1-NG material, which showed lowest activity, had also the smallest amount of pyridinic nitrogen. It is

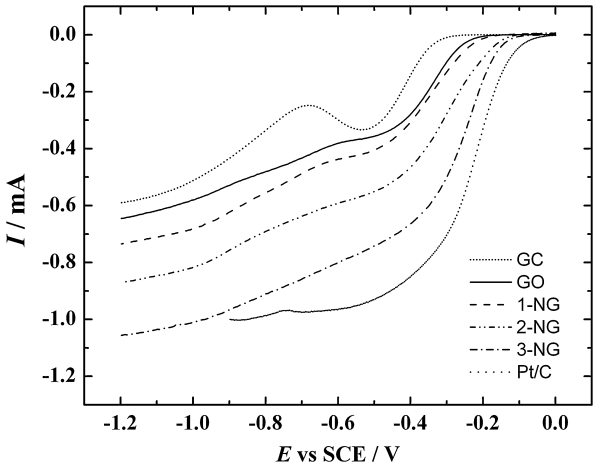

Fig. 5. Comparison of RDE results of oxygen reduction on bare GC, GO/GC, NG/GC and Pt/C modified GC electrodes in O_2-saturated 0.1 M KOH. v = 10 mV s^{-1}, ω = 1900 rpm.

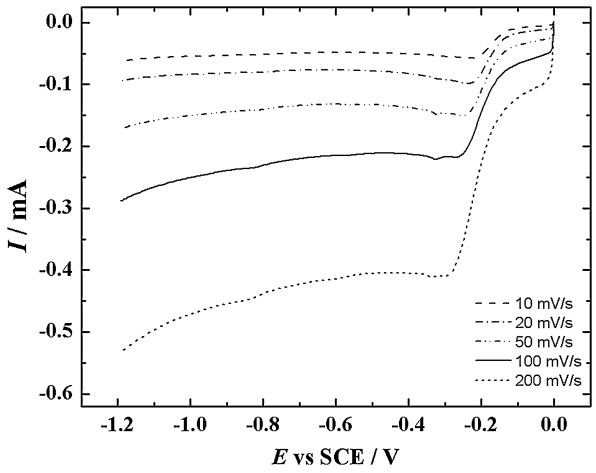

Fig. 6. LSV curves for oxygen reduction on a 3-NG/GC electrode in O_2-saturated 0.1 M KOH. ν = 10–200 mV s^{-1}.

important to note, that at low overpotentials the GO material catalyses a two-electron O_2 reduction, but for NG materials the value of n significantly increases. Several groups have studied the fuel tolerance of NG catalysts for ORR and it was found that NG possesses excellent tolerance to the crossover effect accompanied by high cycling stability [21,27]. As expected, the overall oxygen reduction activity of the Pt/C catalyst is higher than that of NG materials (Fig. 5). However, it needs to be stressed that the difference in the $E_{1/2}$ value between the most active NG catalyst (3-NG) and Pt/C is only ca. 50 mV. This indicates the excellent electrocatalytic activity of 3-NG towards the ORR in alkaline media. These are important results from the point of view of practical application of NG materials as cathode catalysts for low-temperature alkaline membrane fuel cell.

Very recently a hybrid catalyst of nitrogen-doped graphene/carbon nanotubes was prepared by pyrolysis of DCDA in the presence of carbon nanomaterials [49]. This catalyst showed a good electrocatalytic property for ORR in acid media. The ORR activity of undoped catalyst was significantly lower [49]. The type of nitrogen species that is active for ORR might depend on solution pH. Therefore the ORR performance of N-doped nanocarbons is strongly affected by pH [50].

The electrocatalytic property of 3-NG catalyst material was also studied by linear sweep voltammetry (LSV) in O_2-saturated 0.1 M KOH solution. The LSV measurements were carried out using different potential scan rates (10–200 mV s^{-1}). Fig. 6 presents the LSV responses of the 3-NG modified GC electrode in 0.1 M KOH. The O_2 reduction wave of 3-NG has more positive onset potential than that of the GO catalyst (data not shown) and also the peak currents for 3-NG are higher than for GO/GC electrodes, which shows again that N-doping is necessary for an efficient O_2 reduction electrocatalysis to occur. The reduction current peak appeared at a rather positive potential, indicating superior electrocatalytic properties of this NG catalyst. In the next stage of work the most active NG material will be tested in the fuel cell conditions.

4. Conclusions

In this work the electrocatalysis of O_2 reduction on annealed graphene oxide and nitrogen-doped graphene catalysts has been explored. Nitrogen doping was achieved by pyrolysis of GO at 800 °C in the presence of melamine, urea or dicyandiamide. According to the XPS results the nitrogen doping level up to 5 at% was observed. The synthesised NG materials were electrochemically characterised in alkaline media and the RDE and LSV results revealed that these catalysts possess a high electrocatalytic activity towards O_2 reduction. The NG material synthesised in the presence of DCDA showed the best ORR performance. DCDA as a nitrogen precursor is easy to handle (non-flammable), making N-doping method feasible for the preparation of N-containing graphene cathodes for low-temperature fuel cell applications.

Acknowledgements

This research was financially supported by the Estonian Science Foundation (Grant No. 9323) and by the Estonian Nanotechnology Competence Center. We also acknowledge support from the Archimedes Foundation (Project No. 3.2.0501.10-0011).

References

[1] A. Rabis, P. Rodriguez, T.J. Schmidt, ACS Catal. 2 (2012) 864–890.
[2] R. Othman, A.L. Dicks, Z. Zhu, Int. J. Hydrogen Energy 37 (2012) 357–372.
[3] Z.W. Chen, D. Higgins, A.P. Yu, L. Zhang, J.J. Zhang, Energy Environ. Sci. 4 (2011) 3167–3192.
[4] Y.Y. Shao, J.H. Sui, G.P. Yin, Y.Z. Gao, Appl. Catal., B 79 (2008) 89–99.
[5] D.A. Stevens, M.T. Hicks, G.M. Haugen, J.R. Dahn, J. Electrochem. Soc. 152 (2005) A2309–A2315.
[6] S. Wakeland, R. Martinez, J.K. Grey, C.C. Luhrs, Carbon 48 (2010) 3463–3470.
[7] Y. Li, W. Zhou, H. Wang, L. Xie, Y. Liang, F. Wei, J.-C. Idrobo, S.J. Pennycook, H. Dai, Nat. Nanotechnol. 7 (2012) 394–400.
[8] I. Kruusenberg, N. Alexeyeva, K. Tammeveski, Carbon 47 (2009) 651–658.
[9] I. Kruusenberg, N. Alexeyeva, K. Tammeveski, J. Kozlova, L. Matisen, V. Sammelselg, J. Solla-Gullon, J.M. Feliu, Carbon 49 (2011) 4031–4039.
[10] G. Jürmann, K. Tammeveski, J. Electroanal. Chem. 597 (2006) 119–126.
[11] N. Alexeyeva, K. Tammeveski, Electrochem. Solid-State Lett. 10 (2007) F18–F21.
[12] K.S. Novoselov, A.K. Geim, S.V. Morozov, D. Jiang, Y. Zhang, S.V. Dubonos, I.V. Grigorieva, A.A. Firsov, Science 306 (2004) 666–669.
[13] A.K. Geim, K.S. Novoselov, Nat. Mater. 6 (2007) 183–191.
[14] Q. Liu, H. Zhang, H. Zhong, S. Zhang, S. Chen, Electrochim. Acta 81 (2012) 313–320.
[15] L. Sun, L. Wang, C. Tian, T. Tan, Y. Xie, K. Shi, M. Li, H. Fu, RSC Adv. 2 (2012) 4498–4506.
[16] Z. Lei, L. Lu, X.S. Zhao, Energy Environ. Sci. 5 (2012) 6391–6399.
[17] E. Antolini, Appl. Catal., B 123-124 (2012) 52–68.
[18] M.D. Stoller, S. Park, Y. Zhu, J. An, R.S. Ruoff, Nano Lett. 8 (2008) 3498–3502.
[19] C. Soldano, A. Mahmood, E. Dujardin, Carbon 48 (2010) 2127–2150.
[20] S. Stankovich, D.A. Dikin, R.D. Piner, K.A. Kohlhaas, A. Kleinhammes, Y. Jia, Y. Wu, S.T. Nguyen, R.S. Ruoff, Carbon 45 (2007) 1558–1565.
[21] C. Zhu, S. Dong, Nanoscale 5 (2013) 1753–1767.
[22] H. Wang, T. Maiyalagan, X. Wang, ACS Catal. 2 (2012) 781–794.
[23] Z. Yang, H. Nie, X. Chen, X. Chen, S. Huang, J. Power Sources 236 (2013) 238–249.
[24] K. Gong, F. Du, Z. Xia, M. Durstock, L. Dai, Science 323 (2009) 760–764.
[25] Z.H. Sheng, L. Shao, J.J. Chen, W.J. Bao, F.B. Wang, X.H. Xia, ACS Nano 5 (2011) 4350–4358.
[26] Z. Luo, S. Lim, Z. Tian, J. Shang, L. Lai, B. MacDonald, C. Fu, Z. Shen, T. Yu, J. Lin, J. Mater. Chem. 21 (2011) 8038–8044.
[27] Z. Lin, G. Waller, Y. Liu, M. Liu, C.-P. Wong, Adv. Energy Mater. 2 (2012) 884–888.
[28] Y. Sun, C. Li, G. Shi, J. Mater. Chem. 22 (2012) 12810–12816.
[29] L. Qu, Y. Liu, J.-B. Baek, L. Dai, ACS Nano 4 (2010) 1321–1326.
[30] K.R. Lee, K.U. Lee, J.W. Lee, B.T. Ahn, S.I. Woo, Electrochem. Commun. 12 (2010) 1052–1055.
[31] C.-W. Tsai, M.-H. Tu, C.-J. Chen, T.-F. Hung, R.-S. Liu, W.-R. Liu, M.-Y. Lo, Y.-M. Peng, L. Zhang, J. Zhang, D.-S. Shy, X.-K. Xing, RSC Adv. 1 (2011) 1349–1357.
[32] H. Liu, Y. Liu, D. Zhu, J. Mater. Chem. 21 (2011) 3335–3345.
[33] N. Alexeyeva, E. Shulga, V. Kisand, I. Kink, K. Tammeveski, J. Electroanal. Chem. 648 (2010) 169–175.
[34] M. Vikkisk, I. Kruusenberg, U. Joost, E. Shulga, K. Tammeveski, Electrochim. Acta 87 (2013) 709–716.
[35] Z.Y. Lin, M.K. Song, Y. Ding, Y. Liu, M.L. Liu, C.P. Wong, Phys. Chem. Chem. Phys. 14 (2012) 3381–3387.
[36] W.S. Hummers, R.E. Offeman, J. Am. Chem. Soc. 80 (1958) 1339.
[37] V. Datsyuk, M. Kalyva, K. Papagelis, J. Parthenios, D. Tasis, A. Siokou, I. Kallitsis, C. Galiotis, Carbon 46 (2008) 833–840.
[38] H.C. Schniepp, J.L. Li, M.J. McAllister, H. Sai, M. Herrera-Alonso, D.H. Adamson, R.K. Prud'homme, R. Car, D.A. Saville, I.A. Aksay, J. Phys. Chem. B 110 (2006) 8535–8539.
[39] S. Chandra, S. Sahu, P. Pramanik, Mater. Sci. Eng., B Solid 167 (2010) 133–136.
[40] I. Kruusenberg, J. Mondal, L. Matisen, V. Sammelselg, K. Tammeveski, Electrochem. Commun. 33 (2013) 18–22.
[41] F. Lima, G.V. Fortunato, G. Maia, RSC Adv. 3 (2013) 9550–9560.
[42] A.J. Bard, L.R. Faulkner, Electrochemical Methods, second ed., Wiley, New York, 2001.

[43] R.E. Davis, G.L. Horvath, C.W. Tobias, Electrochim. Acta 12 (1967) 287–297.
[44] D.R. Lide, CRC Handbook of Chemistry and Physics, 82nd ed., CRC, Press, Boca Raton, 2001.
[45] J.J. Wu, D. Zhang, Y. Wang, B.R. Hou, J. Power Sources 227 (2013) 185–190.
[46] Y. Zhang, K. Fugane, T. Mori, L. Niu, J. Ye, J. Mater. Chem. 22 (2012) 6575–6580.
[47] S. Ni, Z.Y. Li, J.L. Yang, Nanoscale 4 (2012) 1184–1189.
[48] L.F. Lai, J.R. Potts, D. Zhan, L. Wang, C.K. Poh, C.H. Tang, H. Gong, Z.X. Shen, Y. Lin, R.S. Ruoff, Energy Environ. Sci. 5 (2012) 7936–7942.
[49] C.H. Choi, M.W. Chung, H.C. Kwon, J.H. Chung, S.I. Woo, Appl. Catal. B 144 (2014) 760–766.
[50] W.Y. Wong, W.R.W. Daud, A.B. Mohamad, A.A.H. Kadhum, K.S. Loh, E.H. Majlan, Int. J. Hydrogen Energy 38 (2013) 9370–9386.